

Research Article

TiO₂/SiO₂ Composite Films Immobilized on Foam Nickel Substrate for the Photocatalytic Degradation of Gaseous Acetaldehyde

Hai Hu, Wenjun Xiao, Jian Yuan, Jianwei Shi, and Wenfeng Shangguan

Research Center for Combustion and Environment Technology, Shanghai Jiao Tong University, Shanghai 200240, China

Correspondence should be addressed to Wenfeng Shangguan, shangguan@sjtu.edu.cn

Received 11 July 2007; Revised 26 September 2007; Accepted 10 January 2008

Recommended by Terry Egerton

The photocatalyst anatase titanium dioxide (TiO₂) films were immobilized via sol-gel technique on foam nickel modified with SiO₂ films as transition layer (indicated as TiO₂/SiO₂ films). The structural properties of TiO₂/SiO₂ composite films were characterized using TG-DSC, XRD, FE-SEM, and BET. The photocatalytic activities of immobilized TiO₂/SiO₂ films were tested through photocatalytic degradation reactions of gaseous acetaldehyde under ultraviolet (UV) light irradiation. The substrate modification with transition layer of SiO₂ films improved the specific surface area (SSA) of substrate and the acetaldehyde adsorption on photocatalyst film enormously and resulted in great enhancement of photocatalytic activity and stability. The degradation ratio of gaseous acetaldehyde (concentration of 100 ppmv) on TiO₂/SiO₂ photocatalysts reached 100% after 100 minutes of irradiation. The photocatalytic activity of TiO₂/SiO₂ films reduced about 15% after 9 consecutive runs, which was more stable than that of TiO₂ films, and was completely recovered after heating at 300°C for 1 hour.

Copyright © 2008 Hai Hu et al. This is an open access article distributed under the Creative Commons Attribution License, which permits unrestricted use, distribution, and reproduction in any medium, provided the original work is properly cited.

1. INTRODUCTION

Volatile organic compounds (VOCs) are one of the most important causes of indoor air pollution, and their effective removal has become a focus in the field of indoor air quality (IAQ). Formaldehyde is one of the major indoor VOCs pollutants and exists extensively in modern building materials and furnishings. The removal of formaldehyde is vital for improving IAQ and occupants' health due to the toxic and carcinogenic risks [1].

Photocatalysis, as an environmentally friendly technology, has attracted much attention for its potential application in utilizing the cheap and abundant solar energy. TiO₂ semiconductor is a widely used photocatalyst for the removal of all kinds of organic and inorganic pollutants in air or water because of its stability, nontoxicity, low cost, and a relatively satisfying activity [2–5]. However, TiO₂ suspension system applied in practice often suffers from the aggregation of suspended particles with ultrafine size and the difficulties in separation of photocatalyst from suspension after reaction [6, 7]. Photocatalyst immobilization technology overcomes

the above problems [8–10]. Many materials have been used as supports for photocatalysts such as glass [11], stainless steel [12], porous alumina [13, 14], activated carbon [15, 16], zeolite [17, 18], ceramic foam [19–21], silica gel [22], and so on. All these materials have certain drawbacks such as small SSA, low light transmittance, and so on. Foam metal materials have been recently utilized in heterogeneous catalysis because their uniform open-porous and reticulate structure provides the catalytic system excellent gas-dynamic properties and sufficient contact of the gaseous reactants with the catalyst surface [23], which show significant advantages in gas-phase photocatalytic reactions [24, 25], so they are expected to be utilized as substrate in remediation of indoor air pollution that mainly caused by VOCs.

The immobilization process often results in decrease of photocatalytic activity because of reduction in photocatalyst surface area. Liu et al. [26, 27] used polyvinyl alcohol (PVA) as a binder to immobilize TiO₂ on support, but it might be not stable and could react with positive holes to result in the decrease of photocatalytic activity. So enhancing the photocatalytic activity of immobilized TiO₂ is of great significance

for its application in environmental purification. The combination of TiO_2 and absorbents has been reported to be effective for the enhancement of photocatalytic activity [28, 29]. Our previous studies showed that the preheating treatment of the foam nickel substrate increased its SSA and provided more sites for TiO_2 loading resulting in the enhancement of photocatalytic activity of the immobilized TiO_2 [25]. In the present paper, foam nickel was modified by coating SiO_2 films possessing large SSA and strong adsorbability as transition layers. Anatase TiO_2 films were immobilized on the modified substrate via sol-gel technique without any organic binder. Acetaldehyde was used as a substitute for formaldehyde to test the photocatalytic activity of $\text{TiO}_2/\text{SiO}_2$ films under UV irradiation because it has similar physical and chemical properties and less toxicity than formaldehyde.

The aim of the work reported in this paper was to investigate the effect of SiO_2 transition layers coated on substrate on surface properties and photocatalytic activity of immobilized TiO_2 . The effects of photocatalyst preparation parameters along with their photocatalytic behavior in deactivation and regeneration are presented.

2. EXPERIMENTAL

2.1. Composite $\text{TiO}_2/\text{SiO}_2$ films preparation

All chemicals were of analytical grade, provided by China Medicine (Group) Shanghai Chemical Reagent Corporation, and were used without any treatment. Precursor solutions for SiO_2 and TiO_2 films were prepared via sol-gel processes. SiO_2 sol was prepared as follows: Ethyl silicate (TEOS) was dissolved in anhydrous ethanol under stirring for 1 hour at room temperature, and then the mixture of deionized water and hydrochloric acid was added dropwise into the solution under vigorous stirring. The resultant precursor solution was stirred at room temperature for 1 hour, and then was sealed and placed in the dark for 24 hours. Finally, a uniform, stable, and transparent sol of SiO_2 was obtained through above procedure. The final mole ratio of HCl, TEOS, $\text{C}_2\text{H}_5\text{OH}$, and H_2O was 0.05 : 1 : 2 : 10 in the sol. The synthetic procedure of TiO_2 sol was described in earlier literature [25]. Foam nickel wafer (thickness of *ca.* 1.4 mm, porosity $\geq 95\%$, and $\text{Ni} \geq 99.9 \text{ wt.}\%$) was used as basic substrate materials. After ultrasonic treatment in ethanol to remove grease, the foam nickel was washed with distilled water and dried at room temperature.

SiO_2 and TiO_2 films were prepared by a dip-coating method. A piece of predried foam nickel was dipped in the SiO_2 sol for minutes and then rotated at high speed to form a wet gel film. After drying at room temperature for 12 hours, the sample was calcined at 450°C for 2 hours in an air flow oven. TiO_2 films were deposited according to the same procedure instead of calcining at 550°C for 1 hour. The $\text{TiO}_2/\text{SiO}_2$ double-layer films were prepared by coating SiO_2 layer on foam nickel firstly, then depositing TiO_2 layer over the SiO_2 layer. For comparison, the onefold TiO_2 films immobilized on foam nickel were synthesized as reported in earlier literature [25], in which the foam nickel was preheated at 550°C for 10 minutes before coating TiO_2 films.

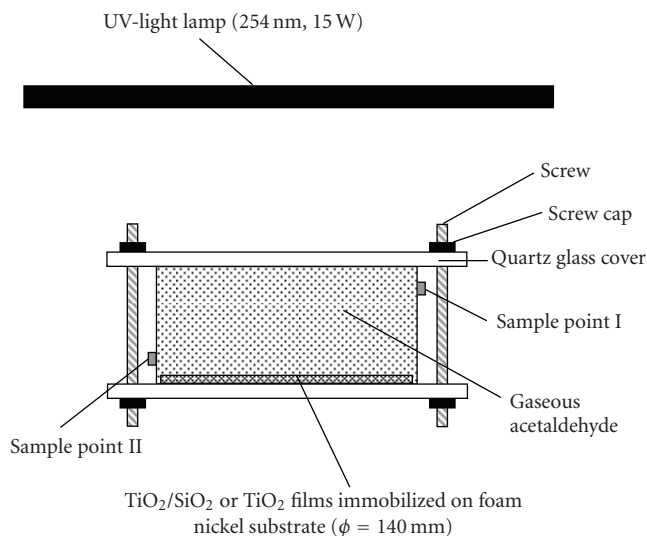


FIGURE 1: Schematic diagram of photoreactor for acetaldehyde photocatalytic degradation.

The operations of dipping, drying, and heating in air were repeated several times in order to obtain TiO_2 , SiO_2 , and $\text{TiO}_2/\text{SiO}_2$ films coated on foam nickel with various coating cycles. The prepared TiO_2 , SiO_2 , and $\text{TiO}_2/\text{SiO}_2$ films will be denoted as T1, T2, S1, S2, S1T1, S1T2, S2T1, and S2T2, where T and S indicate TiO_2 and SiO_2 , respectively, and the numbers followed indicate the coating cycles of the films. The arrange order of T and S expresses the deposition order of TiO_2 and SiO_2 films. No obvious changes in adhesion properties of the prepared films immobilized on foam nickel wafer and mechanical properties of foam nickel were observed after calcination in the study.

2.2. Photocatalyst characterization

The thermal gravimetric and differential scanning calorimetry (TG-DSC) curves were recorded using a TGA 2050 thermogravimetric analyzer (TA instruments, USA) and a DSC 404/LF instrument (Netzsch, Germany). The TiO_2 and SiO_2 gel powders were heated in an air atmosphere by a temperature raise of $10^\circ\text{C}/\text{min}$, which was the same heating condition as the preparation of TiO_2 and SiO_2 films. The X-ray diffraction (XRD) patterns were recorded using an X-ray diffractometer (Bruker, D8 ADVANCE) operated at 40 kV and 40 mA utilizing a $\text{Cu K}\alpha$ radiation source ($\lambda = 0.15405 \text{ nm}$). The surface morphology was observed using a field-emission scanning electron microscope (FE-SEM; Sirion 200, Philips). The SSA and the pore-size distribution were determined by multipoint Brunauer-Emmett-Teller (BET) method and Barrett-Joyner-Halenda (BJH) procedures (Quantachrome Instruments, NOVA 1000). The samples of TiO_2 , SiO_2 , or $\text{SiO}_2/\text{TiO}_2$ films coated on foam nickel were cut into small pieces before the BET and BJH measurements.

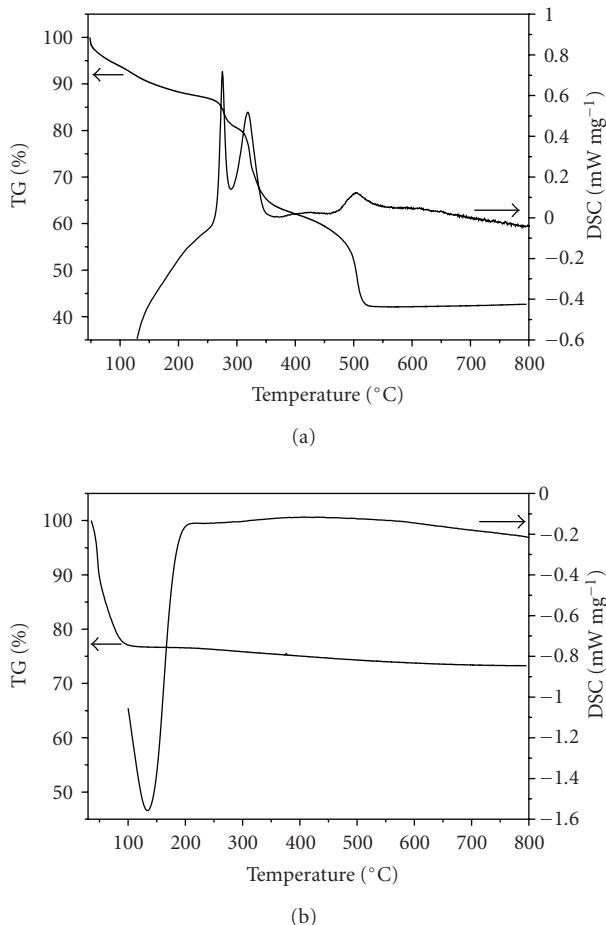


FIGURE 2: TG-DSC curves of the room-temperature-dried TiO_2 (a) and SiO_2 (b) gels in an air atmosphere.

2.3. Photocatalytic activity tests

The photocatalytic activity of prepared materials was evaluated by photocatalytic degradation of gaseous acetaldehyde. The process of photocatalytic oxidation of acetaldehyde was conducted in a cylindrical glass reactor, which was provided with a quartz window of ca. 167.3 cm^2 and a volume of 1000 cm^3 . The scheme of the photoreactor is presented in Figure 1. The initial concentration of gaseous acetaldehyde (from Guang Ming Special Gas Co. Ltd., Dalian) injected into the reactor was ca. 100 ppmv (parts per million by volume). The photocatalyst immobilized on foam nickel substrate ($\phi = 140 \text{ mm}$) was placed on the reactor bottom and was irradiated by a 15 W UV-light lamp with dominant emission at 254 nm through the quartz window after the adsorption equilibrium of gaseous acetaldehyde was reached. The bare-foam nickel and foam nickel coated with SiO_2 films were used for blank test. The vertical distance between light source and photocatalyst was 25 cm. The average light intensity striking on the film surface was about $400 \mu\text{W cm}^{-2}$, as measured by a UV radiometer (made in the Photoelectric Instrument Factory of Beijing Normal University) with the peak intensity of 254 nm. The concentrations of acetaldehyde

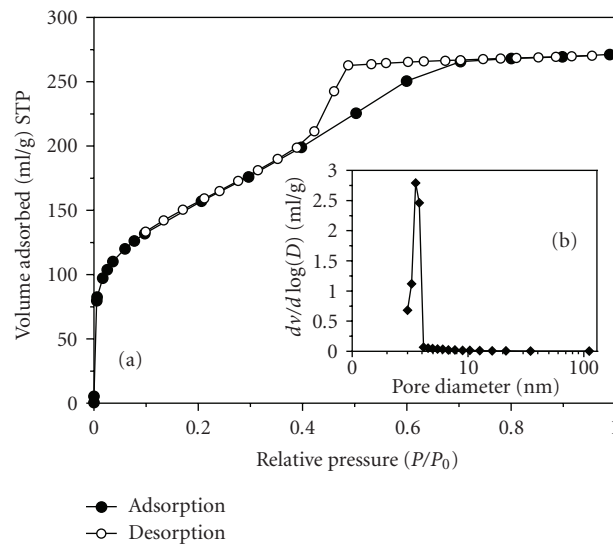


FIGURE 3: N_2 adsorption-desorption isotherms (a) and pore-size distribution (b) of SiO_2 powder obtained from sol-gel method.

and CO_2 in gas phase were measured by a gas chromatograph (model GC9160, Ouhua instruments, Shanghai) equipped with a Porapak-R column ($2.0 \text{ m} \times 3.0 \text{ mm}$) and a flame ionization detector (FID) after converting CO_2 to CH_4 through a Ni-catalyst methanizer. The temperatures of the Porapak-R column and methanizer were 100°C and 360°C , respectively. Nitrogen was used as the carrier gas.

3. RESULTS AND DISCUSSION

3.1. Characterization of $\text{TiO}_2/\text{SiO}_2$ composite photocatalyst

Figure 2 shows the TG-DSC thermograms of the room-temperature-dried TiO_2 and SiO_2 gels in an air atmosphere by heating at the rate of $10^\circ\text{C}/\text{min}$ to 800°C . In Figure 2(a), the weight loss of TiO_2 gel ended before heating in 520°C . The exothermic peak at 514°C may be assigned to the phase transition of amorphous TiO_2 to anatase TiO_2 . Therefore, the calcination temperature for TiO_2 films was selected at 550°C in order to get the anatase TiO_2 films with large SSA. In Figure 2(b), the only obvious weight loss process of SiO gel ended before heating in 100°C , which was assigned to evaporation of H_2O in the gel. No exothermic or endothermic peak was observed, indicating that no phase transition of SiO_2 occurred, and only amorphous SiO_2 was generated below 800°C . The synthetic conditions for SiO_2 films were selected at 450°C for 2 hours.

Figure 3 shows the nitrogen adsorption-desorption curves measured by BET method and the pore-size distribution calculated from desorption isotherms of SiO_2 powder prepared by sol-gel method. The SiO_2 powder has enormous adsorption ability and a SSA of $550.4 \text{ m}^2 \text{ g}^{-1}$. The pore-size distribution of SiO_2 is very concentrated with an average size of 3.5 nm, belonging to mesoporous materials. The SSAs of bare-foam nickel, S1 and S2 are 0.12, 167.2, and $159.4 \text{ m}^2 \text{ g}^{-1}$, respectively. The great increment in the SSAs of S1 and S2 are

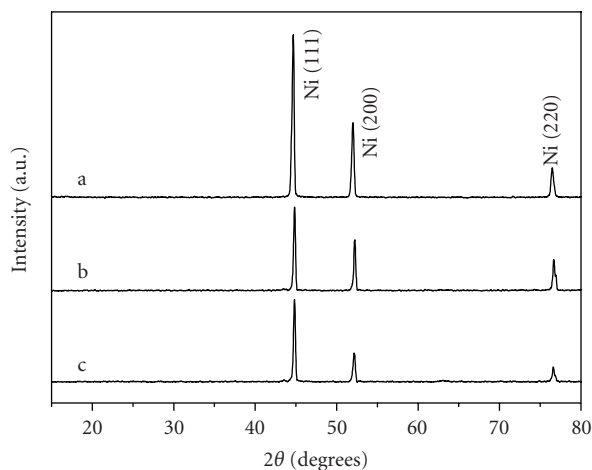


FIGURE 4: XRD patterns of bare-foam nickel (a), S1 (b), and S2 (c).

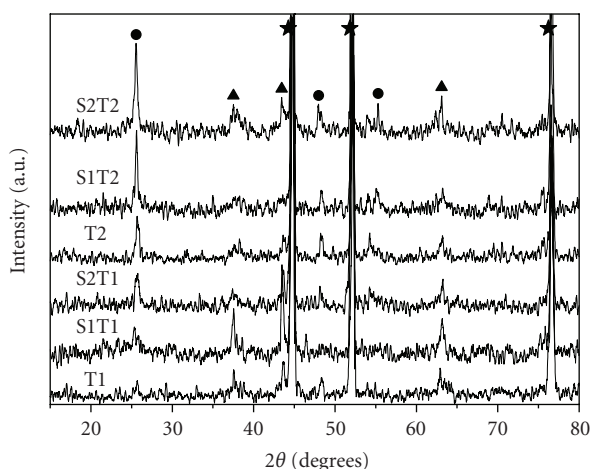
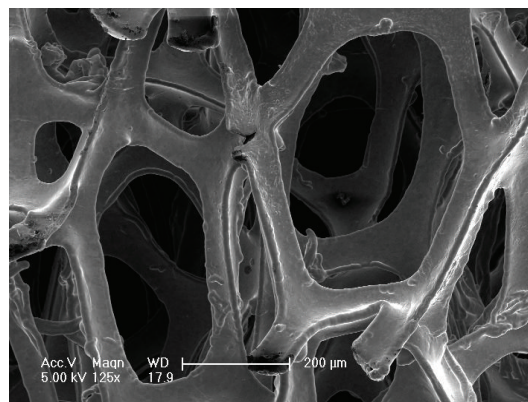


FIGURE 5: XRD patterns of T1, S1T1, S2T1, T2, S1T2, and S2T2. (Symbol: ●—anatase TiO_2 , ▲—NiO, ★—Ni.)

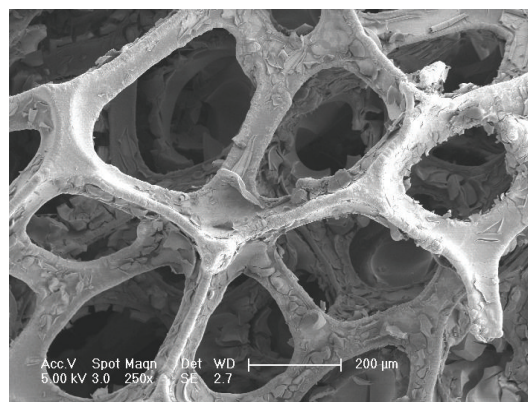
attributed to the coating of SiO_2 possessing large SSA over the foam nickel. However, the repeated heating treatment of S2 resulted in a smaller SSA than the S1. The SiO_2 film loaded on foam nickel as transition layer contributes greatly to providing more active sites on substrate for photocatalyst loading.

Figure 4 shows the XRD patterns of foam nickel substrates that are without modification and modified by SiO_2 films for various coating cycles. The diffraction peaks of Ni (JCPDS file no. 04-0850) but not those of SiO_2 are observed, which indicate the generation of amorphous SiO_2 films. The diffraction intensity of Ni decreases with increasing coating cycles of SiO_2 because the X-ray detection of nickel is hindered by the SiO_2 films coated on it. The weight-increment ratios of SiO_2 for S1 and S2 (i.e., the percentage of the weight of loaded SiO_2 compared with the weight of foam nickel) are 19.4 wt.% and 34.8 wt.%, respectively.

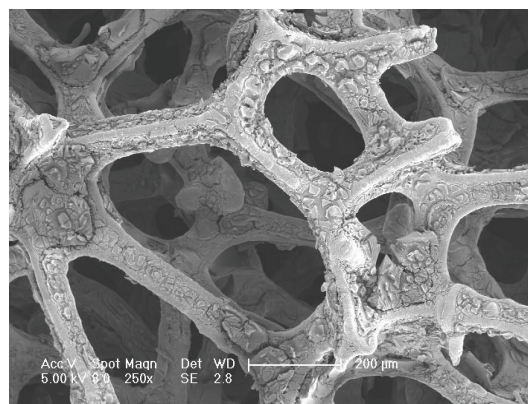
Figure 5 shows the XRD patterns of immobilized photocatalysts of T1, S1T1, S2T1, T2, S1T2, and S2T2. The diffrac-



(a)



(b)



(c)

FIGURE 6: FE-SEM images of bare-foam nickel (a), S2 (b), and S2T2 (c). The scale is 200 μm .

tion peaks of anatase TiO_2 (JCPDS file no. 21-1272) increase with increasing TiO_2 coating cycles, and appear clearly at the second coating cycle. Loading the SiO_2 transition layer also results in peak intensity enhancement of anatase TiO_2 indicating the amount increase of loaded TiO_2 . Slight diffraction peaks of NiO (JCPDS file no. 47-1049) generated from the oxidation of nickel during the calcination are also observed.

TABLE 1: Comparison of surface characteristics and photocatalytic behaviors of various TiO₂ and TiO₂/SiO₂ films immobilized on foam nickel.

Sample	Surface characteristics			Degradation ratio of acetaldehyde in
	SSA of modified substrate (m ² g ⁻¹) ^a	SSA of the sample (m ² g ⁻¹)	TiO ₂ weight ratio (%) ^b	90 min (%) ^c
T1	0.24	0.7	5	35
T2	0.24	0.9	8	62
S1T1	167.2	70.6	4.2	42
S1T2	167.2	35.4	6.6	70
S2T1	159.4	56.0	4.1	80
S2T2	159.4	32.9	7.8	92

^aThe foam nickel substrate was modified by preheating treatment (550°C for 10 minutes) for T1 and T2, and coating SiO₂ as transition layer for S1T1, S1T2, S2T1, and S2T2 before loading TiO₂. The S1 was regarded as modified substrate for S1T1 and S1T2, and S2 as that of S2T1 and S2T2.

^bCalculated according to $R = (W_t/W_{ms}) \times 100\%$, where R is the weight-increment ratio of TiO₂, W_t denotes the weight of loaded TiO₂, and W_{ms} is the weight of modified substrate.

^cGaseous acetaldehyde in 100 ppmv of 1000 cm³. A UV-light lamp ($\lambda = 254$ nm, 15 W) was applied as light source.

The FE-SEM images (Figure 6) display little difference in the framework of substrate among S2, S2T2, and bare-foam nickel, but the surface of S2 and S2T2 is rougher than that of bare-foam nickel after coating SiO₂ and TiO₂ films and heating treatment at high temperature. The weight-increment ratios of TiO₂ for S1T1 and S1T2 are 4.2 wt.% and 6.6 wt.%, respectively (see Table 1), which indicate that the amount of loaded TiO₂ increases with increasing coating cycles of TiO₂. The SSAs of S1T1, S1T2, S2T1, and S2T2 are 70.6, 35.4, 56, and 32.9 m²g⁻¹, respectively. The major distribution ranges of pore size are 3–5 nm for S1 and S2, and 3–10 nm for S1T1, S1T2, S2T1, and S2T2.

3.2. Photocatalytic activity test

3.2.1. Acetaldehyde adsorption

As shown in Figure 7, the TiO₂/SiO₂ composite films have intense adsorption for gaseous acetaldehyde at the initial stage and reach adsorption equilibrium in about 90 minutes after injecting gaseous acetaldehyde into the reactor. The residual concentrations of acetaldehyde in gas phase for TiO₂ films and TiO₂/SiO₂ films are about 70 ppmv and 10 ppmv, respectively. The TiO₂/SiO₂ films have much higher adsorbability for gaseous acetaldehyde than TiO₂ films. It has been reported that the adsorbability of adsorbent used in photocatalytic reaction had much influence on the reaction rate, and the highest reaction rate was achieved by supports that had moderate adsorbability, where a high amount of absorbed reactants is available and could be easily transferred to the loaded TiO₂ particles [28, 29].

3.2.2. Acetaldehyde photocatalytic degradation

The degradation ratios of gaseous acetaldehyde were calculated according to the equation,

$$R_t = \frac{C_t}{C_i}, \quad (1)$$

where R_t is the degradation ratio of gaseous acetaldehyde, C_i denotes the initial concentration of gaseous acetaldehyde

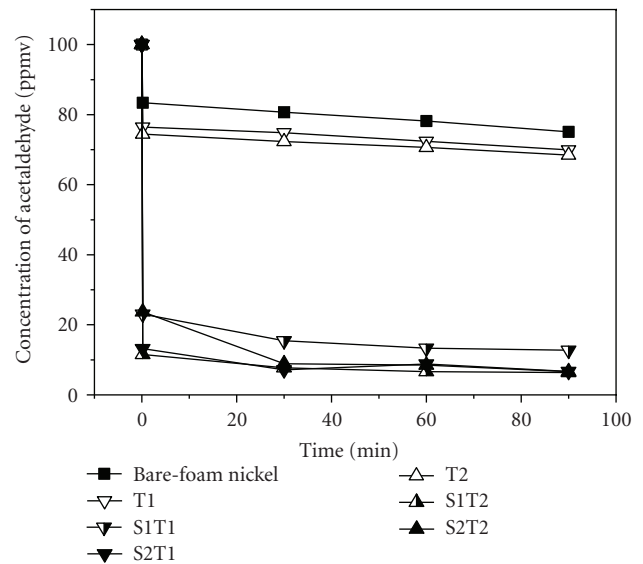


FIGURE 7: Time courses of concentrations of gaseous acetaldehyde caused by adsorption on bare-foam nickel, T1, T2, S1T1, S1T2, S2T1, and S2T2.

(100 ppmv), and C_t is the concentration of completely decomposed acetaldehyde during the reaction calculated from the amount of CO₂ evolution (the complete photocatalytic decomposition of one acetaldehyde molecule yields two carbon dioxide molecules) measured by a gas chromatograph. The degradation plots were the average of three parallel tests.

Blank reactions were performed in the dark or without TiO₂ (i.e., using the substrate samples) under the same experimental conditions of the irradiation experiments. Negligible degradation of acetaldehyde was observed in the absence of TiO₂ or UV irradiation.

Figure 8 presents the photocatalytic decomposition of gaseous acetaldehyde on TiO₂ and TiO₂/SiO₂ films immobilized on foam nickel under UV light irradiation. The degradation ratios of gaseous acetaldehyde increase very fast at the beginning of irradiation and then level off. The

photocatalytic activity at the initial stage of reaction is in following order: S2T2 > S1T2 > S2T1 > T2 > S1T1 > T1, while the photocatalytic activity of complete oxidation for total acetaldehyde shows the following order: S2T2 > S2T1 > S1T2 > S1T1 > T2 > T1. The degradation rate of acetaldehyde on onefold TiO₂ films decreases with the irradiation more rapidly than TiO₂ films combining with SiO₂ transition layer. The photocatalytic activity of TiO₂ was observably enhanced by coating SiO₂ films as transition layer. Coating the SiO₂ and TiO₂ films repeatedly was also advantageous to enhance the photocatalytic activity. The complete photocatalytic decomposition of acetaldehyde was achieved after 100 minutes of UV irradiation on S2T2, which was 3.6 times faster than that of S1T1.

From the results of adsorption (Figure 7) and photocatalytic reactions (Figure 8), it is found that the TiO₂/SiO₂ films show higher adsorbability and degrade acetaldehyde more rapidly than the TiO₂ films with the same TiO₂ coating cycles. For instance, the sample S2T1 decomposes acetaldehyde completely after 115 minutes of UV irradiation, which is more than 3 times faster than T1. As well known, the photocatalytic reaction occurs on the surface of photocatalyst, and the photogenerated electrons and holes recombine very fast, so the separation of interfacial charge carrier becomes possibly more effective when the donor or acceptor is preadsorbed before the photocatalytic reaction. The SiO₂ transition layer has a moderate adsorbability to form a relatively higher-concentration environment of gaseous acetaldehyde around TiO₂, and then transfers the acetaldehyde molecules rapidly to TiO₂ films, thus results in a high photocatalytic degradation rate.

3.2.3. Deactivation and regeneration of the photocatalyst

In order to evaluate the stability of photocatalyst, consecutive photocatalytic reactions for acetaldehyde degradation were carried out. As shown in Figures 9 and 10, the photocatalytic activities of T2 and S2T2 films decrease gradually in subsequent runs. However, the deactivation of T2 is faster than that of S2T2. It has been reported that the intermediates of photocatalytic reaction adsorbed on the surface of photocatalyst would depress the photocatalysis process [30]. The larger surface area of S2T2 provides more active sites for photocatalytic reaction, which reduces the ratio of active sites occupied by adsorption of reaction intermediates such as acetic acid, and so on. Nevertheless, the complete reactivations of T2 and S2T2 films were achieved by heating them at 300°C for 1 hour, no visible deactivation caused by the exfoliation of photocatalyst during the reactions was observed.

3.2.4. Reaction mechanism for acetaldehyde photocatalytic degradation

It is known that the basic process of photocatalysis consists of UV light ($\lambda < 380$ nm) exciting an electron from the valence band (VB) to the conduction band (CB) of the TiO₂ semiconductor creating a hole in the valence band. The electron-hole pairs, after migrating to the surface, can

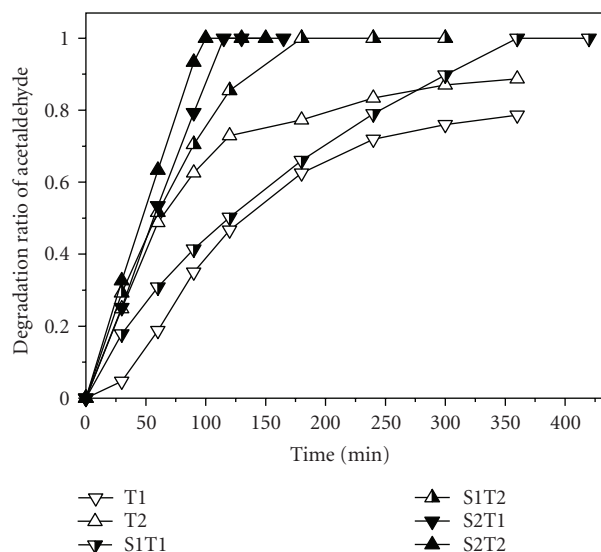


FIGURE 8: Time courses of the photocatalytic decomposition of gaseous acetaldehyde over various TiO₂ and TiO₂/SiO₂ films immobilized on foam nickel under UV-light irradiation ($\lambda = 254$ nm, 15 W).

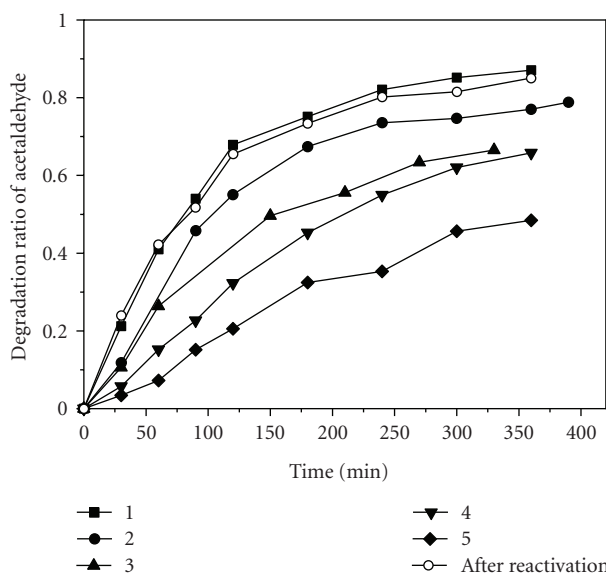


FIGURE 9: Gaseous acetaldehyde degradation rates on T2 for five consecutive runs and regenerated T2 (heating at 300°C for 1 hour) under UV-light irradiation ($\lambda = 254$ nm, 15 W).

in turn be trapped by surface-adsorbed molecules at different sites, leading to oxidation and reduction processes. Under the experimental conditions in this study (weak UV-illumination intensity), most of the adsorbed acetaldehyde molecules should be oxidized to acetic acid firstly. Then, the acetic acid is oxidized into carbon dioxide and water with further illumination. The oxidative photodegradation

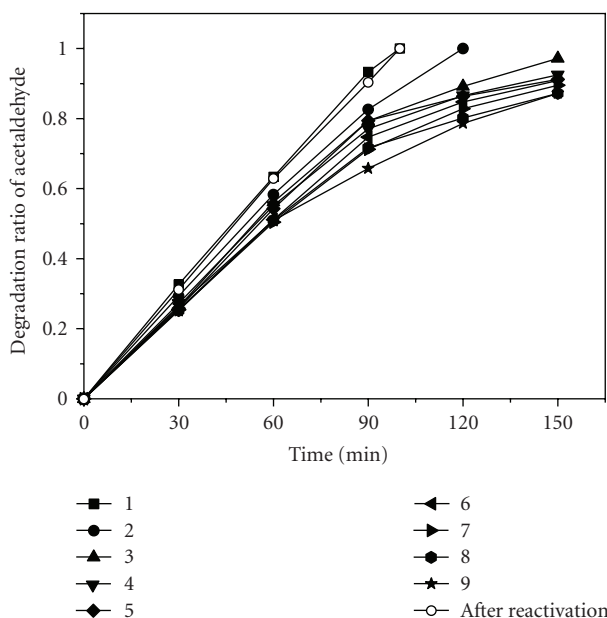


FIGURE 10: Gaseous acetaldehyde degradation rates on S2T2 for nine consecutive runs and regenerated S2T2 (heating at 300°C for 1 hour) under UV-light irradiation ($\lambda = 254$ nm, 15 W).

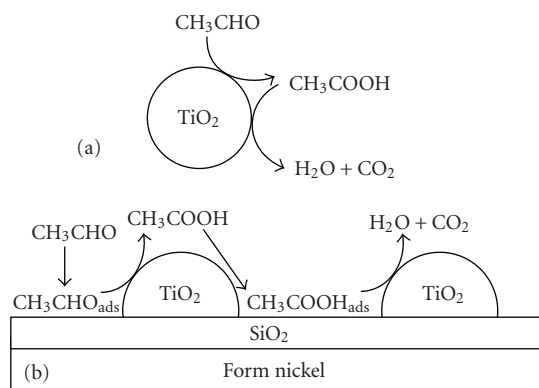
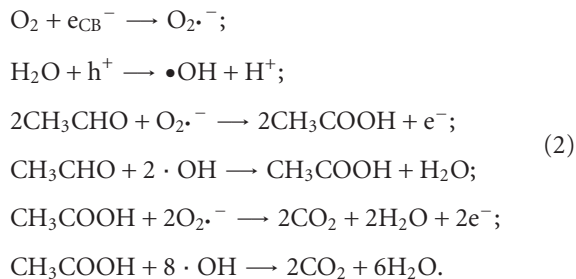


FIGURE 11: Schematic diagram of acetaldehyde photocatalytic decomposition on TiO_2 (a) and $\text{TiO}_2/\text{SiO}_2$ (b) films.

process of acetaldehyde on TiO_2 in principle is described as follows [30]:



It has been established that the adsorbability of photocatalyst is an important factor to determine its decomposition kinetics. In cases of pollutants at low concentrations

of ppmv level, it usually takes long time to complete their decomposition [18, 31]. As for the as-prepared TiO_2 and $\text{TiO}_2/\text{SiO}_2$ films, a considerable part of target reactants and reaction intermediates are adsorbed around the surface of $\text{TiO}_2/\text{SiO}_2$ films, while most parts of them are dispersed in the gas phase on TiO_2 films (Figure 11). It can be concluded that the SiO_2 interlayer has a large capability of collecting target substances and degradation intermediates from the gas phase onto the TiO_2 films, thereby improves the photocatalytic reaction rate.

4. CONCLUSIONS

$\text{TiO}_2/\text{SiO}_2$ films were immobilized on foam nickel substrate by sol-gel technique. The photocatalytic activity and stability of TiO_2 were greatly enhanced by coating SiO_2 films as transition layer. The SiO_2 transition layer possessed large SSA and the $\text{TiO}_2/\text{SiO}_2$ composite film showed much stronger adsorption of gaseous acetaldehyde than the onefold TiO_2 film. The repeated coating of SiO_2 transition layer and TiO_2 photocatalyst increased the amount of TiO_2 immobilized on substrate, which was helpful for accelerating the photocatalytic reaction. It was suggested that the use of inert transition layer possessing large SSA and appropriate adsorbability on support was favorable for enhancing the activity of immobilized TiO_2 photocatalyst.

ACKNOWLEDGMENTS

The study was supported by the Special Foundation of Nanometer Technology (no. 0552nm002), from Shanghai Municipal Science and Technology Commission (STCSM), and National Basic Research Program of China (973 Program no. 2007CB613305).

REFERENCES

- [1] I. M. Ritchie and R. G. Lehnen, "Formaldehyde-related health complaints of residents living in mobile and conventional homes," *American Journal of Public Health*, vol. 77, no. 3, pp. 323–328, 1987.
- [2] W. Bahnemann, M. Muneer, and M. M. Haque, "Titanium dioxide-mediated photocatalysed degradation of few selected organic pollutants in aqueous suspensions," *Catalysis Today*, vol. 124, no. 3-4, pp. 133–148, 2007.
- [3] M. R. Hoffmann, S. T. Martin, W. Choi, and D. W. Bahnemann, "Environmental applications of semiconductor photocatalysis," *Chemical Reviews*, vol. 95, no. 1, pp. 69–96, 1995.
- [4] M. A. Fox and M. T. Dulay, "Heterogeneous photocatalysis," *Chemical Reviews*, vol. 93, no. 1, pp. 341–357, 1993.
- [5] H. S. Hafez, A. El-Hag Ali, and M. S. A. Abdel-Mottaleb, "Photocatalytic efficiency of titanium dioxide immobilized on PVP/AAC hydrogel membranes: a comparative study for safe disposal of wastewater of Remazol Red RB-133 textile dye," *International Journal of Photoenergy*, vol. 7, no. 4, pp. 181–185, 2005.
- [6] J. C. Yu, J. Yu, L. Zhang, and W. Ho, "Enhancing effects of water content and ultrasonic irradiation on the photocatalytic activity of nano-sized TiO_2 powders," *Journal of Photochemistry and Photobiology A*, vol. 148, no. 1–3, pp. 263–271, 2002.

- [7] I. Sopyan, M. Watanabe, S. Murasawa, K. Hashimoto, and A. Fujishima, "A film-type photocatalyst incorporating highly active TiO₂ powder and fluororesin binder: photocatalytic activity and long-term stability," *Journal of Electroanalytical Chemistry*, vol. 415, no. 1-2, pp. 183–186, 1996.
- [8] W. D. Sproul, M. E. Graham, M.-S. Wong, and P. J. Rudnik, "Reactive d.c. magnetron sputtering of the oxides of Ti, Zr, and Hf," *Surface and Coatings Technology*, vol. 89, no. 1-2, pp. 10–15, 1997.
- [9] Q. Zhang and G. L. Griffin, "Gas-phase kinetics for TiO₂ CVD: hot-wall reactor results," *Thin Solid Films*, vol. 263, no. 1, pp. 65–71, 1995.
- [10] J. Yu, X. Zhao, and Q. Zhao, "Effect of surface structure on photocatalytic activity of TiO₂ thin films prepared by sol-gel method," *Thin Solid Films*, vol. 379, no. 1-2, pp. 7–14, 2000.
- [11] K. Akamatsu, A. Kimura, H. Matsubara, S. Ikeda, and H. Nawafune, "Site-selective direct photochemical deposition of copper on glass substrates using TiO₂ nanocrystals," *Langmuir*, vol. 21, no. 18, pp. 8099–8102, 2005.
- [12] L. Zhang, Y. Zhu, Y. He, W. Li, and H. Sun, "Preparation and performances of mesoporous TiO₂ film photocatalyst supported on stainless steel," *Applied Catalysis B*, vol. 40, no. 4, pp. 287–292, 2003.
- [13] K.-S. Hwang, H. Y. Zhu, and G. Q. Lu, "New nickel catalysts supported on highly porous alumina intercalated laponite for methane reforming with CO₂," *Catalysis Today*, vol. 68, no. 1–3, pp. 183–190, 2001.
- [14] Z. Ding, X. Hu, P. L. Yue, G. Q. Lu, and P. F. Greenfield, "Synthesis of anatase TiO₂ supported on porous solids by chemical vapor deposition," *Catalysis Today*, vol. 68, no. 1–3, pp. 173–182, 2001.
- [15] F. L. Y. Lam and X. Hu, "A new system design for the preparation of copper/activated carbon catalyst by metal-organic chemical vapor deposition method," *Chemical Engineering Science*, vol. 58, no. 3–6, pp. 687–695, 2003.
- [16] H. Uchida, S. Itoh, and H. Yoneyama, "Photocatalytic decomposition of propylamide using TiO₂ supported on activated carbon," *Chemistry Letters*, vol. 22, no. 12, pp. 1995–1998, 1993.
- [17] P. Atienzar, A. Corma, H. García, and J. C. Scaiano, "Diffuse reflectance laser flash photolysis study of titanium-containing zeolites," *Chemistry of Materials*, vol. 16, no. 6, pp. 982–987, 2004.
- [18] S. Sampath, H. Uchida, and H. Yoneyama, "Photocatalytic degradation of gaseous pyridine over zeolite-supported titanium dioxide," *Journal of Catalysis*, vol. 149, no. 1, pp. 189–194, 1994.
- [19] J. T. Richardson, M. Garrait, and J.-K. Hung, "Carbon dioxide reforming with Rh and Pt-Re catalysts dispersed on ceramic foam supports," *Applied Catalysis A*, vol. 255, no. 1, pp. 69–82, 2003.
- [20] Y. Peng and J. T. Richardson, "Properties of ceramic foam catalyst supports: one-dimensional and two-dimensional heat transfer correlations," *Applied Catalysis A*, vol. 266, no. 2, pp. 235–244, 2004.
- [21] F.-C. Buciuman and B. Kraushaar-Czarnetzki, "Preparation and characterization of ceramic foam supported nanocrystalline zeolite catalysts," *Catalysis Today*, vol. 69, no. 1–4, pp. 337–342, 2001.
- [22] N. T. Dung, N. V. Khoa, and J.-M. Herrmann, "Photocatalytic degradation of reactive dye RED-3BA in aqueous TiO₂ suspension under UV-visible light," *International Journal of Photoenergy*, vol. 7, no. 1, pp. 11–15, 2005.
- [23] A. N. Pestryakov, V. V. Lunin, A. N. Devochkin, L. A. Petrov, N. E. Bogdanchikova, and V. P. Petranovskii, "Selective oxidation of alcohols over foam-metal catalysts," *Applied Catalysis A*, vol. 227, no. 1-2, pp. 125–130, 2002.
- [24] L. Yang, Z. Liu, J. Shi, Y. Zhang, H. Hu, and W. Shangguan, "Degradation of indoor gaseous formaldehyde by hybrid VUV and TiO₂/UV processes," *Separation and Purification Technology*, vol. 54, no. 2, pp. 204–211, 2007.
- [25] H. Hu, W. Xiao, J. Yuan, J. Shi, M. Chen, and W. Shang Guan, "Preparations of TiO₂ film coated on foam nickel substrate by sol-gel processes and its photocatalytic activity for degradation of acetaldehyde," *Journal of Environmental Sciences*, vol. 19, no. 1, pp. 80–85, 2007.
- [26] H. Liu, S. Cheng, J. Zhang, C. Cao, and S. Zhang, "Titanium dioxide as photocatalyst on porous nickel: adsorption and the photocatalytic degradation of sulfosalicylic acid," *Chemosphere*, vol. 38, no. 2, pp. 283–292, 1999.
- [27] W. Leng, H. Liu, S. Cheng, J. Zhang, and C. Cao, "Kinetics of photocatalytic degradation of aniline in water over TiO₂ supported on porous nickel," *Journal of Photochemistry and Photobiology A*, vol. 131, no. 1–3, pp. 125–132, 2000.
- [28] N. Takeda, T. Torimoto, S. Sampath, S. Kuwabata, and H. Yoneyama, "Effect of inert supports for titanium dioxide loading on enhancement of photodecomposition rate of gaseous propionaldehyde," *Journal of Physical Chemistry*, vol. 99, no. 24, pp. 9986–9991, 1995.
- [29] N. Takeda, M. Ohtani, T. Torimoto, S. Kuwabata, and H. Yoneyama, "Evaluation of diffusibility of adsorbed propionaldehyde on titanium dioxide-loaded adsorbent photocatalyst films from its photodecomposition rate," *Journal of Physical Chemistry B*, vol. 101, no. 14, pp. 2644–2649, 1997.
- [30] I. Sopyan, M. Watanabe, S. Murasawa, K. Hashimoto, and A. Fujishima, "An efficient TiO₂ thin-film photocatalyst: photocatalytic properties in gas-phase acetaldehyde degradation," *Journal of Photochemistry and Photobiology A*, vol. 98, no. 1-2, pp. 79–86, 1996.
- [31] T. Torimoto, S. Ito, S. Kuwabata, and H. Yoneyama, "Effects of adsorbents used as supports for titanium dioxide loading on photocatalytic degradation of propylamide," *Environmental Science and Technology*, vol. 30, no. 4, pp. 1275–1281, 1996.



Hindawi

Submit your manuscripts at
<http://www.hindawi.com>

